Radiative lifetimes of metastable states of negative ions

Pontus Andersson,[1] Karin Fritioff,[1] Joakim Sandström,[1] Gerard Collins,[1] Dag Hanstorp,[1] Anna Ellmann,[2] Peter Schef,[2] Peter Lundin,[2] Sven Mannervik,[2] Peder Royen,[2] K. Charlotte Froese Fischer,[3] Fabian Österdahl,[4] Danijela Rostohar,[5] David J. Pegg,[6] N. D. Gibson,[7] Håkan Danared,[8] and Anders Källberg[8]

[1]*Department of Physics, Göteborg University, SE-412 96 Göteborg, Sweden*

[2]*Department of Physics, Stockholm University, AlbaNova, SE-106 91 Stockholm, Sweden*

[3]*Department of Computer Science, Vanderbilt University, Nashville, Tennessee 37235, USA*

[4]*Department of Physics, Royal Institute of Technology, AlbaNova, SE-106 91 Stockholm, Sweden*

[5]*Institut de Physique Nucléaire, Atomique et de Spectrocopie, Sart Tilman B15, B-4000 Liège, Belgium*

[6]*Department of Physics, University of Tennessee, Knoxville, Tennessee 37996, USA*

[7]*Department of Physics and Astronomy, Denison University, Granville, Ohio 43023, USA*

[8]*Manne Siegbahn Laboratory, Frescativägen 24, SE-104 05 Stockholm, Sweden*

(Received 6 November 2005; published 3 March 2006)

We present a technique for measuring the radiative lifetimes of metastable states of negative ions that involves the use of a heavy-ion storage ring. The method has been applied to investigate the radiative decay of the $np^3\,{}^2P_{1/2}$ levels of $Te^-(n=5)$ and $Se^-(n=4)$ and the $3p^3\,{}^2D$ state of Si^- for which the $J=3/2$ and $5/2$ levels were unresolved. All of these states are metastable and decay primarily by emission of $E2$ and $M1$ radiation. Multi Configuration Dirac-Hartree-Fock calculations of rates for the transitions in Te^- and Se^- yielded lifetimes of 0.45 s and 4.7 s, respectively. The measured values agree well with these predicted values. In the case of the ^2D state of Si^-, however, our measurement was only able to set a lower limit on the lifetime. The upper limit of the lifetime that can be measured with our apparatus is set by how long the ions can be stored in the ring, a limit determined by the rate of collisional detachment. Our lower limit of 1 min for the lifetime of the ^2D state is consistent with both the calculated lifetimes of 162 s for the $^2D_{3/2}$ level and 27.3 h for the $^2D_{5/2}$ level reported by O'Malley and Beck and 14.5 h and 12.5 h, respectively, from our Breit-Pauli calculations.

DOI: 10.1103/PhysRevA.73.032705 PACS number(s): 32.80.Gc, 32.70.Cs

I. INTRODUCTION

In general, a measurement of the radiative lifetime of an excited state involves studying the evolution of the population of the state. The lifetime can be extracted from the resulting exponential decay curve. In the case of ions, one common method is to extract the ions from a source and focus and accelerate them to form a monoenergetic and unidirectional beam. In the beam-foil method [1,2], for example, the ions of the beam are nonselectively excited at a well-defined time by passing them through a thin foil. Since the ions move at a constant velocity, their temporal decay is converted into a spatial decay behind the foil. If the excited state decays via electric-dipole ($E1$) emission, it has a lifetime that is typically a few nanoseconds. In this case the rate of decay is sufficient to allow one to passively monitor the population change by studying the spatial decrease in intensity of the emitted radiation over a relatively short distance. The beam-foil method has essentially been replaced by the beam-laser method [3,4] in which the ions are selectively excited by a laser beam instead of a foil.

For metastable states, which decay by the emission of higher-order radiation such as $E2$ or $M1$, these methods, however, become impractical. The decay of such long-lived states is difficult to track using a linear accelerator and a time-of-flight method since the lifetimes usually translate to many hundreds of kilometers and the light emission intensity from the decay will be vanishingly small. For metastable states with lifetimes in the microsecond range or longer, trapping of ions in either ion traps or storage rings [5] presents a more convenient way of tracking the change in population of such states. In an ion storage ring, which is essentially a circular accelerator, one could, in principle, monitor the population of a metastable state of an ion for infinitely long times after injection into the ring since the ions would circulate forever. In practice, however, collisions with the residual gas in the ring neutralize the ions and limit the time that they can be stored. Nevertheless, storage times can be sufficiently long to track the decay of metastable states of both positive and negative ions.

A convenient way of investigating the decay of a metastable state of an ion in a ring is to actively sample the population as a function of time after injection. Most often, a probe laser is used to selectively excite ions from the metastable state in order to determine the instantaneous population of the state at the time the probe laser is applied. This probing is repeated at different times after excitation to map out the exponential decay curve. Mannervik [6] developed a laser-probing method to measure the radiative lifetimes of metastable states of positive ions. A magnetic storage ring was used to create a circulating beam of positive ions. Radiation from a laser was directed along one straight section of the ring where the ion velocity is locally changed in order to Doppler tune the ions into resonance in front of a photo detector. The laser is used to excite ions from the metastable state to a short-lived, more highly excited state. The prompt fluorescence emitted in the decay of the latter state is used to monitor the time dependence of the population of the metastable state. A decay curve for the metastable state is accu-

mulated by measuring this prompt fluorescence as a function of time after the ions are injected into the ring. The probe pulse is achieved by the use of a mechanical shutter synchronized with the timing of the storage ring. The shutter is sequentially opened to let the laser light into the ring at different delay times from the ion injection. The method has been successfully used to measure lifetimes of metastable positive ions ranging from 3 ms to 28 s [7–9].

Negative ions differ intrinsically from atoms and positive ions since electron correlation plays a more enhanced role in determining their structure and dynamics. As a result of the short-range nature of the force binding the outermost electron, a negative ion has a structure consisting of, typically, only one bound state. The possibility of excited bound states of negative ions, however, was discussed more than three decades ago by Massey [10]. To date, with one exception [11], only excited states with the same electronic configuration, and therefore parity, as the ground state have been observed. Consequently, traditional spectroscopic techniques involving allowed transitions between bound states are not possible in the case of negative ions. The metastability of bound excited states of negative ions accounts for the lack of emission spectra.

Even though there are few bound states in negative ions, there are many excited quasibound states that are embedded in the detachment continuum [12,13]. In general, such states, which are associated with multiple excitation or core excitation, decay rapidly by the process of autodetachment induced by the Coulomb interaction between the electrons. However, in a few cases, a state in the detachment continuum of a negative ion can be metastable. Then the preferred mode of decay is autodetachment via a forbidden process that is induced by the weaker magnetic interactions. Decay by autodetachment produces neutral particles. The lifetime of the metastable state can then be determined by simply counting the number of neutral particles detected as a function of time after the ions are injected into a storage ring. This technique has been applied, for example, to study the lifetimes of metastable states of the He^- [14] and Be^- [15] ions. In other ions, radiative $E1$ transitions have been observed to occur between doubly excited states in the continuum that are metastable against autodetachment [16–20].

Theoretical studies of metastable states of heavy negative ions involve relativistic as well as correlation effects. In the case of a negative ion, there are at least two different types of bound excited states that are metastable against radiative decay. For some ions, the lowest-energy electronic configuration can couple to produce more than one bound state. Each of these states is characterized by a different term value. For example, ions with np^3 configurations couple to excited ^2D and ^2P terms, in addition to the ground-state ^4S term. The excited states ^2D and ^2P states radiatively decay to the ^4S ground state of the same parity primarily via $E2$ and $M1$ transitions. This is the situation for Si^-, which is one of the ions investigated in this work. More generally, the higher-lying levels of the fine-structure multiplet of the ground state are metastable since they can only decay radiatively to lower-lying levels of the same multiplet. This case is represented in the present work by Te^- and Se^- ions with a np^5 configuration. Again, this involves $E2$ and $M1$ transitions since both levels have the same parity. There is, however, an important difference in the decay of ions with configurations of np^3 and np^5. In the latter case, the transition between the $^2P_{1/2}$ and $^2P_{3/2}$ levels is "spin allowed." In the former case, the transition between the $^4S_{3/2}$ and $^2D_{3/2,5/2}$ states is "spin forbidden." Furthermore, the case of the np^3 configurations is special in that, generally, the larger spin-orbit interactions are between the $^4S_{3/2}$ and $^2P_{3/2}$ and between the $^2D_{3/2}$ and $^2P_{3/2}$ levels. Therefore the $^2P_{3/2}$ component in the ground-state wave function largely determines the transition rate. The lifetimes of metastable states of ions that decay via intercombination processes involving spin-forbidden $E2$ and $M1$ transitions are expected to be long.

In an earlier paper [21] we published the result of a measurement and a calculation of the radiative lifetime of the excited $^2P_{1/2}$ state in Te^-. In this paper we more thoroughly present the results of measurements and calculations of the lifetimes of metastable states of the Te^- ion and of two additional ions Se^- and Si^-. Specifically, we have studied the lifetimes of the excited $J=1/2$ levels of the ground-state term $np^5\,^2P$ for $Se^-(n=4)$ and $Te^-(n=5)$. The excited $J=1/2$ level decays to the $J=3/2$ level by emission of $E2$ and $M1$ radiation. In the case of Si^-, we investigated the decay of the metastable ^2D term. We were unable to resolve the fine-structure levels in this measurement. The excited ^2D term decays to the ground-state ^4S term by the emission of $E2$ and $M1$ radiation. Calculations of the forbidden $E2$ and $M1$ decay rates that determined the lifetimes of all these metastable states were performed to complement the experiments.

In order to measure the radiative lifetimes of metastable states of negative ions, we have developed a technique similar in concept to that used by Mannervik to study positive ions [6]. Negative ions, however, differ structurally from positive ions, and this requires a different approach to probing the excited state and to treating a substantial background associated with the neutralization of the ions in collisions with the residual gas in the ring. The method of inducing prompt fluorescence cannot be applied in the case of negative ions since the bound states are not connected optically via allowed radiative transitions. Instead, we have studied the time dependence of the decay in population by selectively photodetaching the ions in the metastable state. Changes in the yield of neutrals produced by photodetachment were used as a monitor of population changes due to the radiative decay. In some aspects this method is also similar to the approach suggested in an article by Balling *et al.* [22]. It is a very powerful method since the neutralized ions leave the ring in a beam and can be monitored with high efficiency. Negative ions are, however, more weakly bound than positive ions and are therefore more readily neutralized in collisions with particles of the residual gas in the ring. Collisions compete with radiative decay in the depopulation of a metastable state. They also lead to a redistribution of populations of the ground and excited states. The neutrals produced in collisional detachment are the source of a significant background in studies of negative ions. The collisional detachment rate, in fact, determines how long negative ions can be stored in the ring and, therefore, the upper limit to the radiative lifetime that can be measured. As we shall see, the present method is applicable if the radiative lifetime

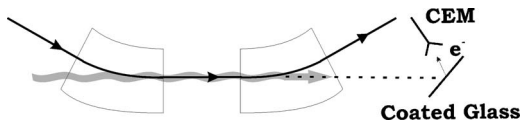

FIG. 1. A schematic of the interaction and detection regions showing the straight flight path between the two bending magnets. The ions circulating in the ring are represented by the solid black line; the laser light is represented by the grey arrow. Fast-moving neutralized atoms, denoted by the dashed line, impinge on the coated glass plate. The secondary electrons that are subsequently emitted are detected with the CEM.

is shorter than the maximum ion storage time, as determined by collisional detachment.

II. EXPERIMENTAL PROCEDURE

The experiments were performed at the heavy-ion storage ring CRYRING situated at the Manne Siegbahn Laboratory in Stockholm [23]. The negative ions were produced in both the ground state and bound excited states in a sputter ion source. The success of the present method relies on the fact that the environment in the source creates a population distribution between ions in the ground and excited states that is not in equilibrium with the thermal environment in the ring. After being accelerated to an energy of typically 30 keV, the ions were injected into the storage ring. The probe laser beam was aligned along one of the 4.3-m-long straight sections of the ring so that it merged collinearly with the ion beam, as shown in Fig. 1. The wavelength of the laser was chosen to selectively photodetach ions in the excited state, while leaving those in the ground state unperturbed. A neutral-particle detector [24] was placed in the tangential arm of the ring after the laser-ion interaction region. The detector counted the number of ions that were neutralized in the interaction region. Ions in all states were neutralized by collisions with the residual gas while only excited state ions where neutralized by the photons. The fast neutral particles impinged on the glass plate which was coated with a thin layer of In_2O_3:Sn. Secondary electrons emitted from the coating were detected with a channel electron multiplier (CEM). The coating served to prevent the glass plate from becoming electrically charged. The signal in the experiments was the number of neutral particles reaching the detector when the laser was turned on for a fixed time period.

For each ring cycle, consisting of injection, acceleration, storing, and dumping of the ion beam, the laser beam was turned on by opening a computer-controlled mechanical shutter at different times after injection ($t=0$) to track the evolution of the population of the metastable state. Since the probe laser affects the population of the excited state, the laser was turned on only once per ring cycle, at different delay times in each cycle. A generic timing diagram is shown in Fig. 2. It should be noted that only the extra signal on top of the background in the figure is due to photodetachment. The background must be subtracted to get the signal that is proportional to the population of the excited level. In order to obtain data of high statistical quality, the signal was accumulated over many ring cycles. As a result it was necessary to normalize the signal with respect to the number of excited ions injected into the ring in each cycle. This was achieved by applying a short (10 ms) laser pulse in the beginning of each cycle. The increase in signal during this pulse was proportional to the initial population of the metastable state. This pulse was made sufficiently short to ensure that the population of the metastable state was not depleted appreciably during the time the probe pulse was applied. Figure 3 illustrates the technique by showing data from Si^-. Area D is the signal obtained for the short laser pulse used for normalization while area A is the time interval used to determine the level of population after the actual delay time. The areas $B1$, $B2$, and C are used to determine the background for collisional neutralization. Thus the photodetachment signal is $[A-(B1+B2)/2]$, while C and D are used for normalization (a correction that is usually negligible).

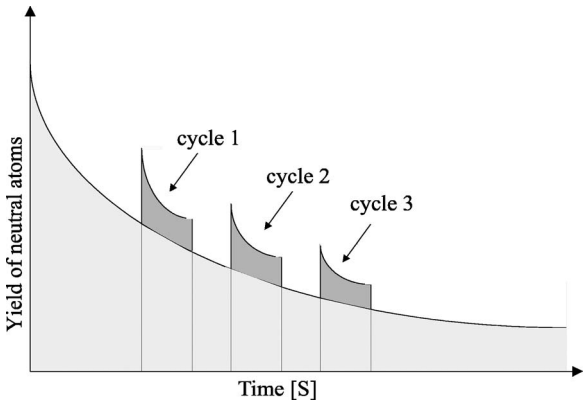

FIG. 2. A generic timing diagram for the experiment. The light-grey area represents the collisional detachment contribution to the neutral-atom signal. The dark-grey areas show the contribution due to the photodetachment of ions in the excited state for three separate ring cycles.

The primary source of background in the experiment was neutrals produced from negative ions in collisions with residual gas particles. Negative ions in both the excited and ground states were detached in this manner. The decay rate was different for ions of different species and depends on the detachment cross section and the pressure in the ring. Colli-

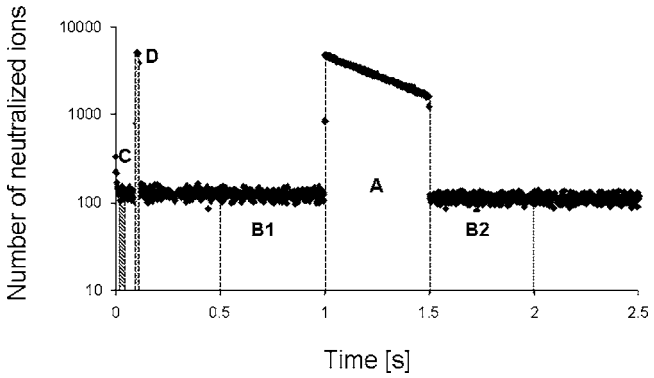

FIG. 3. Experimental data from Si^- illustrating how data were extracted in order to determine the population decay of the excited level as explained in the text.

sional detachment decay curves were accumulated with the laser turned off. Collisions of the ions with the residual gas in the ring can, in addition to causing detachment, also redistribute the populations between the ground and excited states. This process was investigated in the following manner. Just after the injection of the ions into the ring, laser light was applied for a time sufficient to completely deplete the population of the excited state by photodetachment. When the laser is subsequently turned off, the population in the excited state starts to build up again via repopulation from the ground state. This buildup can be probed with the same technique used to investigate the radiative decay of the excited state [25].

A typical decay curve consists of a set of data points, each representing the number of neutrals detected at a given time after injection, corrected for the collisional detachment contribution. This quantity is proportional to the population of the metastable state and of the number of ions in the ring at a given time after injection. The repopulation of the metastable state caused by collision with rest gas in the ring is, at equilibrium, proportional to the (decaying) intensity of the ion beam in the ring. In general, the extracted decay curves were found to be the sum of two exponentials. The faster-decaying component corresponds to the decay of the metastable state, and the longer component is associated with the intensity of the ion beam and collisions that redistribute the populations of metastable and ground states.

The decay rate extracted for the metastable state is mainly due to the radiative decay, but collisional detachment will also contribute. In order to determine the contribution of the collisional detachment effect for the metastable state, we accumulated decay curves at several different ring pressures. In the present work, we used either three or four different pressures, the highest being about a factor of 4 greater than the lowest pressure, which was the normal residual pressure in the ring. The pressure change is accomplished by controlled heating of a vacuum pump in one section of the ring. The decay of the ion beam due to collisions with background gas was carefully measured at each pressure, and the rate of this decay was used to establish a relative pressure scale. Uncertainties in this measurement contribute to the error estimate in the final lifetime values. We then used the pressure-dependent radiative decay rates that were extracted from the two-exponential fits to the decay curves and the relative pressures extracted from the stored lifetime of the beam to form a Stern-Vollmer plot. An extrapolation of the best linear fit to the data points at the different pressures allowed us to determine the zero-pressure intercept. At the zero-pressure limit, the radiative decay is unperturbed by collisions and the true radiative lifetime of the metastable state can be extracted from the data.

III. RESULTS

The radiative lifetimes of metastable states of three different ions were studied in the experiments described in this paper. In Fig. 4 the relevant metastable and ground states of the investigated Te^-, Se^-, and Si^- ions are shown. The vertical arrows represent photoexcitation. The photon energy is chosen to selectively detach ions in the excited state, while leaving those in the ground state bound. The radiative lifetime of all excited states is determined by rates for forbidden transitions between the excited and ground states.

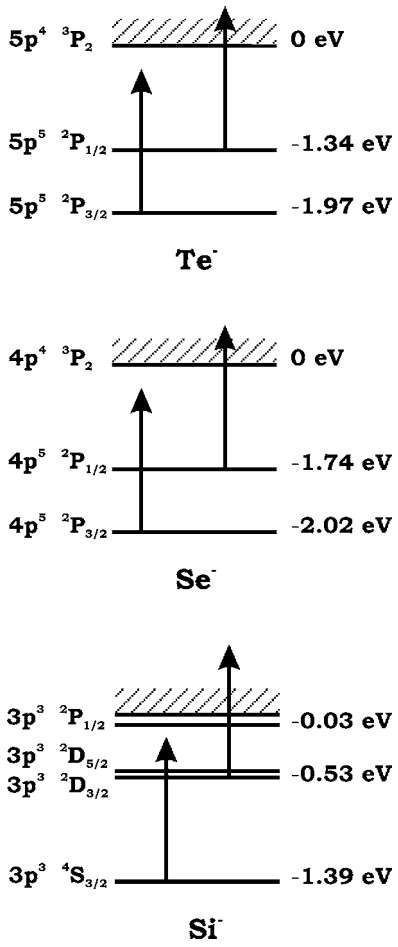

FIG. 4. Energy-level diagrams for the Te^-, Se^-, and Si^- ions showing the metastable excited states and ground states relevant to the present measurements. The vertical arrows represent the photoabsorption. The photon energies are chosen to selectively detach electrons from the excited state ions, leaving ions in the ground state bound.

A. $np^5\ ^2P_{1/2}$ levels of Se^- and Te^-

As can be seen in Fig. 4, the Te^- and Se^- ions consist only of the ground state with its two fine-structure components.

In the case of Te^-, the $J=3/2$ ground state is bound by 1.970 876(7) eV relative to the ground state of the parent Te atom [26]. The excited $J=1/2$ level of the same ^2P term lies 0.620 586 eV [27] above the $J=3/2$ level. Correspondingly, Se^- has an electron affinity of 2.020 67(2) eV and a fine-structure splitting of 0.282 461 eV [27]. The cw radiation used to selectively photodetach ions in the $^2P_{1/2}$ level was produced using a dye laser pumped by an argon-ion laser. The output from the dye laser was typically 1 W, and the power used in the interaction region was approximately 200 mW. The experiment was straightforward. For each ring injection, the laser beam was turned on at different times

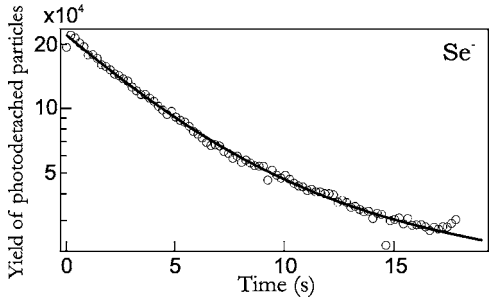

FIG. 5. A semilogarithmic plot of the decay of the $4p^5\,{}^2P_{1/2}$ metastable level in Se^-. The figure shows the number of Se^- ions that were neutralized by photodetachment as a function of time after their injection into the ring. The curve was recorded at the base pressure of the ring. The solid line is the best two-exponential fit to the data.

after injection ($t=0$) to track the evolution of the population of the $J=1/2$ level. Figure 5 shows a measured decay curve of the metastable $J=1/2$ level of the $4p^5\,{}^2P$ term in Se^-. Figure 6 shows the corresponding decay curve of $5p^5\,{}^2P$ term of Te^-.

The solid line shows the best fit to the sum of two exponentials. The exponential with the longer decay constant is associated with the collisional transfer of population between the $J=1/2$ and $J=3/2$ levels. Figure 7 shows the Stern-Vollmer plot of the decay constant measured for Se^- at four different ring pressures that were used to eliminate the effect of collisions. The best linear fit to the data was extrapolated to yield a zero-pressure rate of 0.21 s^{-1}. Correspondingly, the best linear fit to the four data points from our study of Te^- yielded a zero-pressure intercept of 2.38 s^{-1}.

The uncertainties in the lifetime measurements are determined primarily by our ability to accurately determine the zero-pressure intercept. The error in the intercept arises from the extrapolation of the best linear fit through the data points at the four different pressures. This curve-fitting error depends on the statistical quality of the four data points, which represent the pressure-dependent radiative rates. Thus, the error bars on these points originate in the two-exponential

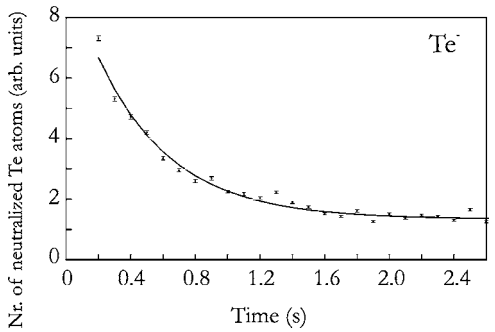

FIG. 6. A plot of the decay of the $5p^5\,{}^2P_{1/2}$ metastable level of Te^-. The figure shows the number of Te^- ions that were neutralized by photodetachment as a function of the time after their injection into the ring. This curve was recorded at the base pressure of the ring. Similar curves were recorded at three other ring pressures. The solid line is the best two-exponential fit to the data. The data were collected during 1500 ring cycles.

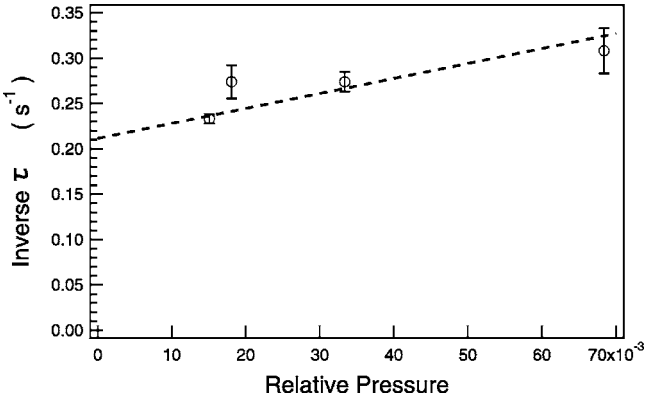

FIG. 7. This Stern-Vollmer plot shows the pressure dependence of the decay rate of the metastable $4p^5\,{}^2P_{1/2}$ level in Se^-. The data points were obtained from the decay curves recorded at four different ring pressures. The solid line represents the best linear fit to the data. The extrapolation of this line to zero pressure yields a radiative lifetime of 4.7 s.

fits to the decay curves taken at each pressure. In general, the larger the difference in the decay constants of the two exponentials, the better the fit and the smaller the error bar on the data points in the Stern-Vollmer plot. This, in turn, allows the extrapolation of the linear fit through the data points to determine the zero-pressure intercept more accurately. We feel that the error on the intercept arising from the fit, which is statistical in origin, is unrealistically small since only four data points are used in the fit. In the case of Se^-, we have estimated more conservative uncertainties in the lifetimes in the following manner. First we noted that the linear fits in the Stern-Vollmer plots showed a relatively weak pressure dependence. Over a change in pressure of a factor of 4, the decay rates only change by about 50% for the Se^- case and 20% in the case of the Te^-. The zero-pressure rate must be lower than the rate at the lowest pressure studied, the base pressure. We have therefore used the upper value of the error bar on the lowest-pressure data point to represent the uncertainty on the zero-pressure intercept. Using this method, we obtain an uncertainty in the decay rate for Se^- of 0.03 s^{-1}. Converting this to lifetime, the experimentally determined lifetime is 4.7 ± 0.7 s. for Se^-. In the case of Te^-, an uncertainty in the decay rate of 0.3 s^{-1} yields a final lifetime value of 0.42 ± 0.05 s.

The results of these measurements are in excellent agreement with value obtained using the Multi Configuration Dirac-Hartree-Fock (MCDHF) formalism that is discussed later in the text.

B. $3p^3\,{}^2D$ term in Si^-

A diode-pumped solid-state cw $Nd:YVO_4$ laser was used to selectively photodetach Si^- ions in the unresolved $J=5/2$ and $3/2$ levels of the ^2D term. It was operated at a fixed wavelength of 1064 nm and had an output power of 4.7 W. Figure 4 shows that the chosen wavelength was sufficient to detach electrons from Si^- ions in the ^2D levels, but not the $^4S_{3/2}$ level. We found this lifetime to be very long, and the best we could do under the circumstances was to

TABLE I. Calculated transition energies E, transition rates A, and radiative lifetimes for Te^-. The length and velocity forms are labeled l and v, respectively.

Calculation	E (cm^{-1})	$A(E2)$ (s^{-1})	$A(M1)$ (s^{-1})	Lifetime (s)
6 (SD)	4957.9	0.00999 (l)	2.1805	0.4565
		0.01155 (v)		
7 (SD)	4966.2	0.01035 (l)	2.1973	0.4537
		0.01099 (v)		
7 (SDTQ)	4966.8	0.01024 (l)	2.1926	0.4540
		0.01089 (v)		

place a lower limit on the lifetime of the ^2D term. Our data indicate that the radiative lifetime of the unresolved $J=5/2$ and $3/2$ levels is longer than 1 min. The subsequent predicted radiative lifetime of the metastable state confirms that the lifetime is far too long to be measured by use of the present method. It is much longer than the storage lifetime of the Si^- ions in the ring, which is determined by collisional detachment.

IV. THEORY

For Te^-, the MCDHF method has been used to calculate the transition probabilities for the higher-order processes of $M1$ and $E2$ decay. In the MCDHF approach, the wave functions are expanded in jj-coupled configuration states and orbital optimization is performed using energy expressions from the Dirac-Coulomb Hamiltonian [28]. The finite size of the nucleus was modeled in the form of an extended Fermi distribution. The core orbitals ($1s$-$4d$, in nonrelativistic terminology) were determined from a multiconfiguration calculation that took into account some of the near degeneracy effects by including $5s^2$-$5d^2$ and $5p^2$-$5d^2$ excitations. The same orbitals were used for both the $J=1/2$ and $3/2$ levels. The correlation model was one in which the outer electrons were assumed to have a $5s^25p^5$ configuration. Both outer-shell correlation from single and double excitations (SD) and core-polarization correlation from $4d^{10}$ were included. Since the principal quantum number has no specific meaning for correlation orbitals, it is convenient to omit the $4f$ orbital. An $n=5$ calculation then determined the $5s$-$5g$ orbitals by optimizing simultaneously on $J=1/2$ and $3/2$ states and keeping the core orbitals fixed. The generalized occupation number for the $5g$ orbital was 0.002. Consequently, no other g orbitals were included. The $n=6$ calculation determined the $6s$-$6f$ orbitals in a similar fashion. Finally, the $7s$-$7f$ orbitals were introduced, but these were optimized separately for the $J=1/2$ and $3/2$ states. Once the orbitals were optimized, the frequency-dependent Breit and QED corrections were included using a configuration interaction calculation for the Dirac-Coulomb-Breit Hamiltonian. Finally, some triple and quadruple excitations (TQ) were added to the expansion. These were obtained as SD excitations from the $5s5p^55d$ and $5s^25p^35d^2$ configurations. These contributions appeared to have negligible effects on the decay rates. In Table I, the excellent stability of the results from the last three calculations is shown. The final value for the $M1$ decay rate is 2.19 s^{-1}. The $M1$ process dominates the $E2$ process in this case, the $E2$ rate being about two orders of magnitude smaller than the $M1$ rate. Thus the final calculated radiative lifetime of the $^2P_{1/2}$ level in Te^- was determined to be 0.45 s.

TABLE II. Comparison of Breit-Pauli lifetime τ for levels of $3p^3$ in Si^- compared with values reported by O'Malley and Beck [29].

	Breit-Pauli	Ref. [29]
$^2D_{3/2}$	14.5 h	162 s
$^2D_{5/2}$	12.2 h	27.3 h
$^2P_{1/2}$	28.1 s	
$^2P_{3/2}$	25.1 s	23.6 s

For Se^-, the MCDHF formalism was again used in the calculation of the rates for the forbidden decay processes that coupled the $J=1/2$ and $3/2$ levels. In this case the calculated $M1$ rate was found to be about three orders of magnitude greater than the $E2$ rate. The final value for the $M1$ rate was 0.203 s^{-1}, which corresponds to a radiative lifetime of the metastable $J=1/2$ level of 4.92 s. The Se^- calculation was not quite as extensive as the Te^- one. In the case of Se^-, the effect of the polarization of the $3d^{10}$ core was excluded since it was expected to be small. Similarly, the Breit correction was not included in the Se^- calculation since it was also expected to make a small contribution.

In both the Te^- and Se^- measurements, the decay rate associated with collisions is much smaller than the radiative decay rate. This made it relatively simple to separate the two depopulation processes using a two-exponential fit to the decay curve. In the case of Si^-, however, this was not the case. O'Malley and Beck [29] have reported lifetimes of 162 s and 27.3 h for the $J=3/2$ and $5/2$ levels of the ^2D state, respectively. In this case, the radiative rate is considerably smaller than the collision rate, and so we can only quote a lower limit on the measured lifetime of the state. In Fig. 4, the ground and excited bound states of Si^- are shown. The electrons in the $3p^3$ configuration of Si^- couple to produce the ^4S, ^2D, and ^2P terms in an L-S coupling scheme. The $^2P_{1/2}$ state is, however, so weakly bound that its presence is not expected to be observed in the measurement. Ions in this state will either be detached due to collisions in the high-temperature environment of the ion source or by blackbody radiation in the initial phase after injection into the ring. Consequently, we studied only the radiative decay of the ^2D term. The $J=3/2$ and $5/2$ levels were not resolved in the measurement. The decay to the ^4S ground state is not allowed in the $E1$ approximation since the upper and lower terms have the same parity. In an attempt to confirm the results reported by O'Malley and Beck, the MCHF formalism was used to determine the rates of decay of the ^2D term via $M1$ and $E2$ radiation [30] with relativistic effects included through the Breit-Pauli Hamiltonian. $E2$ transitions depend strongly on the outer regions of the wave function. Since the negative ion is formed through the attachment of an electron to the neutral atom, our model configuration was $3s^23p^23p'$ where $3p'$ may be quite different from $3p$. In an

TABLE III. $M1$ and $E2$ transition rates (the integers in parentheses are the exponents of powers of 10 that multiply the preceding number) and lifetimes of the $np^5\ ^2P_{1/2}$ levels in O^-, Se^-, Se^-, and Te^-

	Z	$E2(L)$	$E2(V)$	$M1$	Lifetime
$2p^5$	8	1.70(−10)	8.27(−11)	1.38(−4)	2.01 h
$3p^5$	16	6.36(−8)	6.25(−8)	2.29(−3)	7.28 min
$4p^5$	34	1.41(−4)	1.41(−4)	2.03(−1)	4.92 s
$5p^5$	52	1.02(−2)	1.09(−2)	2.19	0.454 s

orthogonal orbital basis this becomes a linear combination of the $3s^23p^3$ and $3s^23p^24p$ configurations. The nonequivalent electron picture allows the $4p$ orbital to have a much larger mean radius than $3p$, appropriate for a negative ion. In the Breit-Pauli approximation, all LS terms with a common J may interact. For $J=3/2$, this includes the $^4S_{3/2}$, $^2D_{3/2}$, and $^2P_{3/2}$ levels and the $^4P_{3/2}$ and $^4D_{3/2}$ levels. Admixtures from the ^4P and ^4D terms contribute directly to $E2$ and $M1$ transitions to the ground state, for which the selection rule (for individual components) requires the same total spin. Calculations were performed for wave function expansions including SD as well as triple (T) and quadruple (Q) excitations, with at most one excitation from the $2p^6$ core. The opening of the $2p^6$ subshell produced no appreciable change in the $M1$ transition probability. The calculated lifetimes of the $^2D_{3/2}$ and $^2D_{5/2}$ levels were not found to be vastly different from each other as found by O'Malley and Beck. In Table II our results are compared with those of O'Malley and Beck. We have compared our calculated energies of the $^2D_{3/2}$ and $^2P_{3/2}$ levels with the accepted experimental values from spectroscopy. The calculated values are higher, but only by 416 cm^{-1} and 766 cm^{-1}, respectively. The calculated energies of O'Malley and Beck are about 700 cm^{-1} and 1500 cm^{-1} higher than the spectroscopic results. Thus correlation has been treated more completely in our case. The Breit-pauli results are not definitive in that they are sensitive to the computational details. We did not, however, find the transition probability for the $M1$ transition to exceed that for the $E2$ transition, $^4S_{3/2}$-$^2D_{3/2}$. Further detailed theoretical studies are clearly needed.

V. DISCUSSION

We have used a storage ring to measure the radiative lifetimes of metastable states in several atomic negative ions. The evolution of the population of the excited state was monitored by applying a probe laser pulse at various times after the ions were injected into the ring. The measured decay rate of the excited state was corrected for depopulation via detachment collisions with the residual gas in the ring. MCDHF and MCHF calculations were performed to determine the expected rates for radiative decay via $M1$ and $E2$ transitions. The experimental method that was used is applicable to many other negative-ion species. In the present experiment, lasers were operated in the visible and IR to selectively photodetach ions in metastable states that are relatively tightly bound. commercially available optical parameter oscillators can currently generate radiation that would be suitable to selectively photodetach metastable states in ions other than those studied in the present work. There are many candidates for such measurements.[31]

Table III shows the results of a MCDHF calculation of $E2$ and $M1$ rates for the decay of the metastable $np^5\ ^2P_{1/2}$ levels of four homologous ions O^-, S^-, Se^-, and Te^-. It can be seen from the table that the $M1$ rate dominates the decay process in all cases. The $E2$ transition energy, however, scales faster with Z than the $M1$ transition energy does. In the Breit-Pauli approximation, the line strength of the $M1$ transition is constant and so the transition rate scales simply as ΔE^3, where ΔE is the transition energy. The $E2$ transition rate, on the other hand, scales as ΔE^5 and the line strength, which is proportional to the transition element $\langle np|r^2|np\rangle$, increases with n. Consequently, the importance of the $E2$ process relative to the $M1$ process increases as the ion becomes heavier.

Our measurements of the lifetime for the $^2P_{1/2}$ levels in Se^- and Te^- are in excellent agreement with the calculations. A measurement on the S^- ion might be possible, but the predicted long lifetime of the metastable level in O^- would be beyond the capabilities of the present technique. The upper limit of a lifetime that can be measured with the method introduced in this paper is set by the stored lifetime of the ions in the ring, a quantity that is determined by the rate of collisional detachment. Thus, for example, in the case of Si^-, we were only able to set a lower limit on the radiative lifetime of the ^2D state because the storage lifetime of Si^- ions in the ring was much shorter than the Breit-Pauli lifetimes of 12–15 h.

ACKNOWLEDGMENTS

This work was supported by the Swedish Research Council and the Wenner-Gren Foundation. The staff at the Manne Siegbahn Laboratory is acknowledged for their support during the experiments. This work was also supported in part by the National Science Foundation under Grant No. 0140233.

[1] L. Kay, Phys. Lett. **5**, 36 (1963).
[2] S. Bashkin, Nucl. Instrum. Methods **28**, 88 (1964).
[3] H. J. Andrä, A. Gaupp, and W. Wittmann, Phys. Rev. Lett. **31**, 501 (1973).
[4] J. Cooper, N. D. Gibson, and J. Lawler, J. Quant. Spectrosc. Radiat. Transf. **1**, 85 (1997).
[5] E. Träbert, Phys. Scr. **T100**, 88 (2002).
[6] S. Mannervik, Phys. Scr. **T105**, 67 (2003).
[7] J. Lindberg, A. Al-Khalili, R. D. Cowan, L.-O. Norlin, P. Royen, and S. Mannervik, Phys. Rev. A **56**, 2692 (1997).
[8] D. Rostohar, A. Derkatch, H. Hartman, S. Johansson, H. Lundberg, S. Mannervik, L.-O. Norlin, P. Royen, and A. Schmitt, Phys. Rev. Lett. **86**, 1466 (2001).
[9] H. Hartman, D. Rostohar, A. Derkatch, P. Lundin, P. Schef, S. Johansson, H. Lundberg, S. Mannervik, L.-O. Norlin, and P. Royen, J. Phys. B **36**, L197L202 (2003).
[10] H. S. W. Massey, *Negative Ions* (Cambridge University Press, London, 1976).
[11] R. Bilodeau and H. K. Haugen, Phys. Rev. Lett. **85**, 534 (2000).
[12] G. Haeffler, I. Y. Kiyan, D. Hanstorp, B. J. Davies, and D. J. Pegg, Phys. Rev. A **59**, 3655 (1999).
[13] I. Y. Kiyan, Phys. Rev. Lett. **84**, 5975 (1998).
[14] U. V. Pedersen, M. Hyde, S. P. Møller, and T. Andersen, Phys. Rev. A **64**, 012503 (2001).
[15] U. V. Pedersen, A. Svendsen, P. Blæsild, and T. Andersen, J. Phys. B **35**, 2811 (2002).
[16] S. Mannervik, G. Astner, and M. Kisielinski, J. Phys. B **13**, L144 (1980).
[17] R. L. Brooks, J. E. Hardis, H. G. Berry, L. J. Curtis, K. T. Cheng, and W. Ray, Phys. Rev. Lett. **45**, 1318 (1980).
[18] J. O. Gaardsted and T. Andersen, J. Phys. B **22**, L51 (1989).
[19] P. Kristensen, V. Petrunin, H. Andersen, and T. Andersen, Phys. Rev. A **52**, R2508 (1995).
[20] V. V. Petrunin, M. Harbst, and T. Andersen, Phys. Rev. A **63**, 030701 (2001).
[21] A. Ellmann *et al.*, Phys. Rev. Lett. **92**, 253002 (2004).
[22] P. Balling, L. Andersen, T. Andersen, H. K. Haugen, P. Hvelplund, and K. Taulbjerg, Phys. Rev. Lett. **69**, 1042 (1992).
[23] K. Abrahamsson *et al.*, Nucl. Instrum. Methods Phys. Res. B **79**, 269 (1993).
[24] D. Hanstorp, Nucl. Instrum. Methods Phys. Res. B **100**, 165 (1995).
[25] J. Lidberg, A. Al-Khalili, L.-O. Norlin, P. Royen, X. Tordoir, and S. Mannervik, Nucl. Instrum. Methods Phys. Res. B **152**, 157 (1999).
[26] G. Haeffler, A. E. Klinkmüller, J. Rangell, U. Berzinsh, and D. Hanstorp, Z. Phys. D: At., Mol. Clusters **38**, 211 (1996).
[27] M. Scheer, R. C. Bilodeau, and H. K. Haugen, J. Phys. B **31**, L11 (1998).
[28] F. A. Parpia, C. F. Fischer, and I. P. Grant, Comput. Phys. Commun. **94**, 249 (1996).
[29] S. M. O'Malley and D. R. Beck, J. Phys. B **36**, 4301 (2003).
[30] G. Tachiev and C. F. Fischer, J. Phys. B **32**, 5805 (1999).
[31] T. Andersen, H. Haugen, and H. Hotop, J. Phys. Chem. Ref. Data **28**, 1511 (1999).